CSIRO PUBLISHING

RESEARCH FRONT

Aust. J. Chem. **2012**, *65*, 905–917
http://dx.doi.org/10.1071/CH12079

Full Paper

Structure Correlation Study of the Beckmann Rearrangement: X-ray Structural Analysis and $^{13}C–^{13}C$ 1-Bond Coupling Constant Study of a Range of Cyclohexanone Oxime Derivatives*

Shin Dee Yeoh,[A] *Benjamin L. Harris,*[A] *Tristan J. Simons,*[A]
and Jonathan M. White[A,B]

[A]School of Chemistry and BIO-21 Institute, University of Melbourne,
Parkville, Vic. 3010, Australia.
[B]Corresponding author. Email: whitejm@unimelb.edu.au

The X-ray structures of a range of oxime derivatives (**1** and **4**), of cyclohexanone and 4-*tert*-butylcyclohexanone, where the electron demand of the oxygenated substituent on the oxime nitrogen (OR) is systematically varied were determined. It was established that as the OR group becomes more electron demanding, then the N–OR bond distance increases, consistent with the early stages of bond breakage. Concomitant with this structural effect was a noticeable closing up of the N1–C1–C2 bond angle, consistent with the early stages of migration of the antiperiplanar carbon onto the nitrogen substituent. These structural effects are consistent with the manifestation of the early stages of the Beckmann rearrangement in the ground state structures of these oxime derivatives. The carbon–carbon bond distances of the participating carbons in this rearrangement, however, did not vary in a systematic way with the electron demand of the OR substituent, suggesting that the structural effects are too small to be detected using X-ray crystallography. However, the $^{13}C–^{13}C$ 1-bond coupling constants, which are sensitive to the effects of hyperconjugation, were shown to vary in a systematic way with the electron demand of the OR substituent. Structural effects in the oxime **5** derivatives of 2,2-dimethylcyclohexanone, a substrate that is prone to Beckmann fragmentation rather than Beckmann rearrangement, were similar but smaller in magnitude.

Manuscript received: 6 February 2012.
Manuscript accepted: 22 March 2012.

Introduction

The early stages of molecular rearrangements are often apparent in the crystal structures of molecules susceptible to that rearrangement. For example, if a particular bond is broken, or if a particular group migrates during the rearrangement, then deviations of bond distances and angles from their 'standard values' along the reaction coordinate are often observed. This is the structure correlation principle,[1] which holds provided the molecule exists in the ground state, in a geometry which is similar to the transition state geometry for the reaction. In this geometry the frontier orbitals whose interactions facilitate the reaction, can mix in the ground state. Since the original publications by Burgi and Dunitz, this principle has been applied to a wide variety of chemical situations, ranging from ligand addition[2] and dissociation reactions[3] of various metal complexes, carbonyl insertion reactions in transition metal carbonyls,[4] nucleophilic addition to metal-coordinated carbonyl groups,[5] rearrangements of pentacoordinate metal complexes,[6] nucleophilic substitution at silicon and germanium,[7] Berry rearrangements within metal clusters,[8] and formation of Lewis acid Lewis base complexes.[9] Pathways for a variety of conformational interconversions have also been mapped out from analysis of closely related crystal structures.[10] Several pericyclic and pseudopericyclic fragmentations have also been studied using this approach, including the retro Diels Alder reaction,[11] and the pericyclic,[12] and pseudopericyclic[13] cheleotropic carbonyl extrusion reactions. Kirby and Jones et al. have used this approach to map out the early stages of unimolecular solvolysis of a variety of substrates.[14]

Kirby et al. reported the crystal structures of a small number of oxime derivatives and showed that the early stages of the Beckmann fragmentation reaction could be discerned from comparisons of the structural parameters between derivatives with varying reactivity.[15] The early stages along the reaction coordinate from the oxime derivative **1** to the intermediate nitrilium cation **2** (Scheme 1) is achieved by increasing the electron demand of the OR substituent. Structural effects that arise with increasing electron demand of the OR substituent include; (i) lengthening of the N–OR bond distance, (ii) closing of the *anti* C–C–N bond angle (α) from 120° and opening of the *syn* C–C–N bond angle (β) from 120° clearly demonstrating

---

*Dedicated to Allan White on the occasion of his 75th birthday.

the molecular movement associated with migration of the antiperiplanar carbon onto the oxime nitrogen as represented by the transition state **3**. However, systematic effects on the participating, antiperiplanar carbon–carbon bond were not apparent from these studies.

In this paper we extend the structural studies of Kirby et al. to encompass cyclohexanone and 4-*tert*-butylcyclohexanone oximes having leaving groups (OR) encompassing a wider range of reactivities attached to the oxime nitrogen, and determined all the X-ray structures at low temperature. The benefits of carrying out the structure determinations at low temperature are hoped to allow us to measure any smaller, systematic effects on the antiperiplanar carbon–carbon bond involved in the rearrangement. In addition we extended these studies to include, 2,2-dimethylcyclohexanone oxime derivatives, **5**, which have been reported to undergo Beckmann fragmentation[16] (Scheme 2) rather than Beckmann rearrangement under certain conditions, to establish whether increasing the electron demand of the oxime derivative (-OR) would result in different structural effects from those shown by the cyclohexanone oxime derivatives.

Results and Discussion

Cyclohexanone oxime (**1a**) is commercially available, 4-*tert*-butylcyclohexanone oxime (**4a**) was readily prepared from 4-*tert*-butylcyclohexanone by reaction with hydroxylamine hydrochloride, and 2,2-dimethylcyclohexanone was prepared according to a published procedure;[17] purification and conversion to the corresponding oxime derivative **5a** was achieved under standard conditions. The ester and ether derivatives of cyclohexanone oxime **1a**–**1j**, 4-*tert*-butylcyclohexanone oxime **4a**–**4j**, and 2,2-dimethylcyclohexanone **5a**–**5h** prepared for this study are summarised in Table 1, along with the pK_a values of the corresponding parent acids which give an indication of the electron demand of the (OR) substituent. The various derivatives were prepared by standard methods.

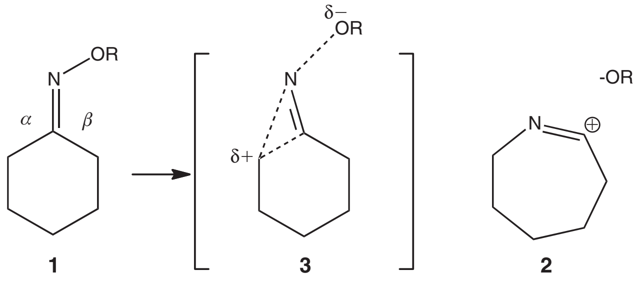

Scheme 1. Beckmann rearrangement of cyclohexanone oxime derivatives.

Crystals suitable for X-ray analysis for **1b**–**1e**, **1g**–**1j**, **4b**, **4d**, **4g**, **5a**–**5c**, **5e**, **5f**, and **5h**, were obtained by slow evaporation from dichloromethane or ether. The picrate derivatives **1i** and **4i** were found to decompose at room temperature but crystals of **1i** suitable for X-ray analysis were obtained by low temperature crystallisation.

The toluene sulphonate ester derivatives **1j** and **4j** were even more reactive, and if crystallised at room temperature Beckmann rearrangement occurred giving the corresponding protonated lactams **6** or **7** as their toluenesulfonate salts (Scheme 3). The structure of **6** was verified by single crystal X-ray diffraction (Fig. 1). Suitable quality crystals of the tosylate derivative of oxime **1j** were eventually grown by crystallisation from dichloromethane within a desiccator at −20°C.

The thermal ellipsoid plots for selected oxime derivatives **1i**, **4b**, and **5b** are presented in Fig. 2 with atom numbering which is representative of all derivatives **1b**–**1e**, **1g**, **1h**, **4b**, **4d**, **4g**, **5a**–**5c**, **5e**, and **5h**. Unfortunately structural analysis of the 3,5-dinitrobenzoate ester **1*e*** showed that the cyclohexane ring is disordered due to the occurrence of two cyclohexane chair conformations at the same molecular site in the crystal.

Table 1. Cyclohexanone oxime derivatives 1a–j, 4a–j, and 5a–h with pK_a values for the corresponding parent acids

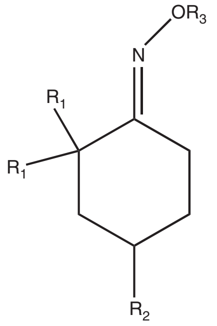

pK_a (ROH)	R_3	$R_1, R_2 = H$	$R_1 = H$ $R_2 = Bu^t$	$R_1 = Me$ $R_2 = H$
16	H	**1a**	**4a**	**5a**
7.15[18]	4-$NO_2C_6H_4$	**1b**	**4b**	**5b**
3.46[18]	3-$NO_2C_6H_4CO$	**1c**	**4c**	**5c**
3.43[18]	4-$NO_2C_6H_4CO$	**1d**	**4d**	**5d**
2.85[19]	3,5-$(NO_2)_2C_6H_3CO$	**1e**	**4e**	**5e**
2.82[19]	3,4-$(NO_2)_2C_6H_3CO$	**1f**	**4f**	**5f**
2.17[18]	2-$NO_2C_6H_4CO$	**1g**	**4g**	**5g**
1.43[19]	2,4-$(NO_2)_2C_6H_3CO$	**1h**	**4h**	**5h**
0.42[18]	2,4,6-$(NO_2)_3C_6H_2$	**1i**	**4i**	
−2.70[20]	4-$CH_3C_6H_4SO_2$	**1j**	**4j**	

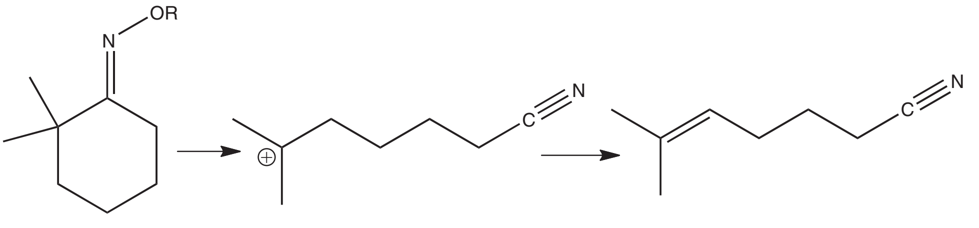

Scheme 2. Beckmann fragmentation of 2,2-dimethylcyclohexanone oxime derivatives.

Molecular parameters derived from disordered structures were deemed unreliable and were not used in this study.

Selected bond distances for the oxime derivatives **1a**–**1d**, **1g**–**1j**, **4b**, **4d**, **4g**, **5a**–**5c**, **5e**, **5f**, and **5h** are presented in Table 2, while selected bond angles and dihedral angles are presented in Table 3. These tables also include data for the related oxime derivatives **8**,[21] and **9**[22] for which the X-ray structures have previously been determined at low temperature.

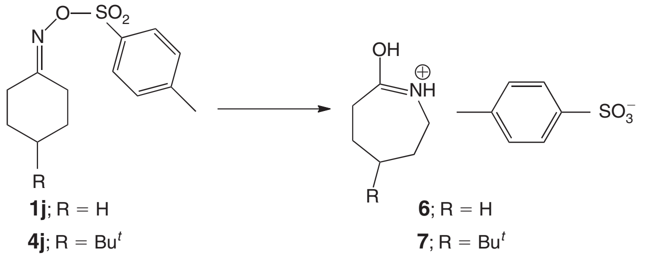

Scheme 3.

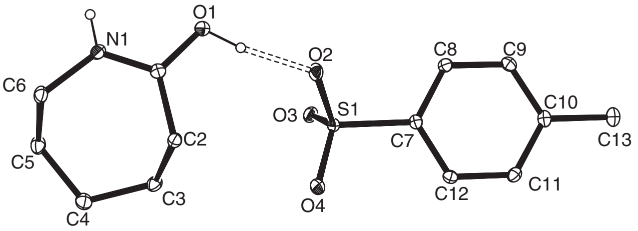

Fig. 1. Thermal ellipsoid plot of the Beckmann rearrangement product **6**.

*Structural Effects in Cyclohexanone Oxime Derivatives **1a**–**1j** and **4b**–**4g***

Inspection of the data contained in Tables 2 and 3 reveals that the C1–N–O bond angle of the oxime moiety is significantly smaller than 120° in all structures with values lying in the range 108.70–109.81°. Although closing of this angle is expected on the basis of VSEPR[24] it also very likely reflects the preference for the non-bonded pair to occupy an orbital with greater *s* character. The data presented in Table 2, also reveals that the N1–OR bond distance lengthens as the electron demand of the OR group increases (as gauged by the pK_a value for the parent acid ROH). This is clearly displayed by the plot of the N1–OR bond distance vs pK_a (ROH), which is presented in Fig. 3 for the cyclohexanone oxime derivatives **1a**–**1j**, **4b**–**4g**, and **8**–**9**. Lengthening of the N1–O1 bond with increasing electron demand can be considered to represent the early stages of the heterolysis of this bond and thus also represents the early stages of the Beckmann rearrangement.

In addition to representing the early stages of the Beckmann rearrangement, the plot in Fig. 3, also represents an application of the *variable oxygen probe*,[25] and as such, the slope is sensitive to the degree of electron donation from both the antiperiplanar (C2–C1) bond and the synperiplanar (C1–C6)

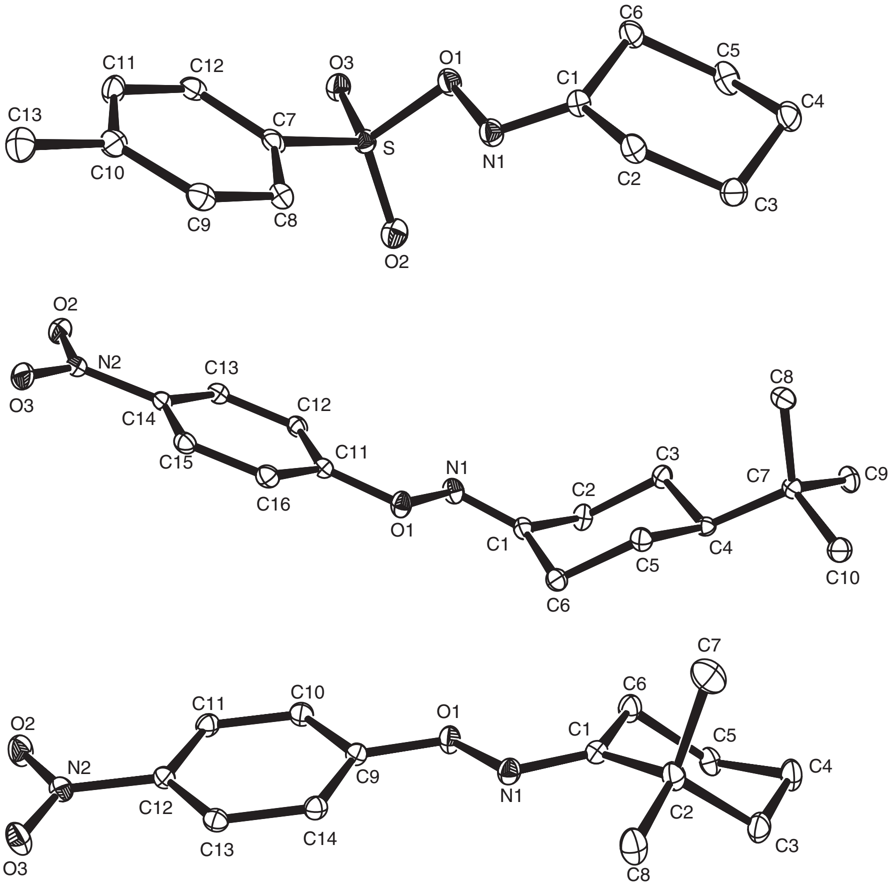

Fig. 2. Thermal ellipsoid plots for oxime derivatives **1j**, **4b**, and **5b**; ellipsoids are at the 20 % probability level.

Table 2. Selected bond distances [Å] for oxime derivatives 1a, 4a, 5a, 8, and 9

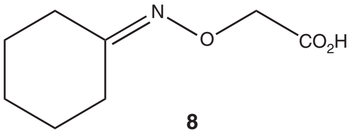

8

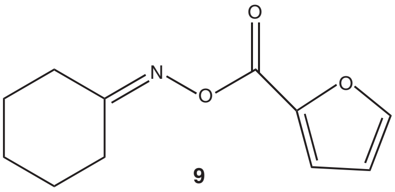

9

	N1–O1	C1–N1	C1–C2	C6–C1	Δ (C1–C2/C1–C6)
1a[23]	1.411(2)	1.280(2)	1.500(2)	1.498(2)	0.002
1b	1.453(2)	1.273(2)	1.508(2)	1.497(2)	0.011
1c	1.442(1)	1.264(2)	1.496(2)	1.487(2)	−0.009
1d	1.467(2)	1.272(2)	1.508(2)	1.501(3)	0.007
1g	1.455(2)	1.278(2)	1.504(2)	1.496(2)	0.008
1h	1.482(2)	1.275(3)	1.504(3)	1.479(3)	0.025
1i	1.479(2)	1.275(2)	1.501(2)	1.502(2)	0.001
1j	1.480(5)	1.280(7)	1.489(7)	1.483(7)	0.006
4b	1.445(2)	1.283(2)	1.497(3)	1.491(2)	0.006
4d	1.455(1)	1.277(2)	1.500(2)	1.497(2)	0.003
4g	1.464(1)	1.274(2)	1.501(2)	1.500(2)	0.001
5a	1.416(2)	1.273(2)	1.520(2)	1.510(2)	0.010
5b	1.441(1)	1.279(2)	1.522(2)	1.507(2)	0.015
5c	1.455(2)	1.277(2)	1.523(2)	1.509(2)	0.014
5e	1.465(2)	1.280(2)	1.521(2)	1.506(2)	0.015
5f	1.456(1)	1.275(2)	1.522(1)	1.503(2)	0.019
5h	1.460(3)	1.284(3)	1.520(3)	1.513(4)	0.007
8	1.433(2)	1.277(2)	1.502(2)	1.502(2)	0.000
9	1.459(2)	1.280(2)	1.509(2)	1.503(2)	0.006

bond into the N–OR antibonding orbital. The σ_{C-C}–σ^*_{N-O} interaction between the anti carbon–carbon bonding orbital and the N–OR antibonding orbital should be significantly stronger that the σ_{C-C}–σ^*_{N-O} interaction involving the *syn* carbon–carbon bond. It is worthwhile making comparison with the corresponding plot of the C–OR bond distance vs pK_a (ROH) for equatorial cyclohexane derivatives **10**,[26] which measures the strength of electron donation from the two antiperiplanar ring carbon–carbon bonds into the C–OR antibonding orbital (Fig. 4). Although there is slightly more scatter in the plot of N–OR bond distance vs pK_a (ROH) shown in Fig. 3 it is clear that there is a significantly stronger response of the N–OR bond distance to the electron demand of the OR substituent in the oxime derivatives **1** (Eqn 2) than in the cyclohexane derivatives **10** (Eqn 1). There are two plausible reasons for this: (*i*) in the oxime derivatives, the σ_{CC}–σ^*_{NOR} interactions are occurring across the C=N double bond whose distance is ~1.276 Å (Table 2). While in derivatives **10**, the σ_{CC}–σ^*_{COR} interactions occur over a C–C single bond with significantly greater distance of ~1.500 Å, there should therefore be a greater orbital overlap and hence a stronger interaction in the former case; (*ii*) in the oximes derivatives, the N–OR antibonding orbital is located on a more electronegative atom (N vs C) hence, the σ^*_{NOR} orbital in the oxime derivatives will have lower energy and interact more strongly with the C–C bonding orbital.

$$\mathbf{10}\text{: } r_{C\text{–}O}\ [\text{Å}] = 1.479 - (2.86 \times 10^{-3})\ \text{p}K_a\ (\text{ROH}) \quad R^2 = 0.97 \tag{1}$$

$$\mathbf{1}\text{: } r_{N\text{–}OR}\ [\text{Å}] = 1.475 - (3.80 \times 10^{3})\ \text{p}K_a\ (\text{ROH}) \quad R^2 = 0.86 \tag{2}$$

Associated with bond lengthening of the N1–OR bond distance as the OR group becomes more electron demanding, is a systematic closing of the N1–C1–C2 bond angle (Fig. 5). This structural effect is consistent with the early stages of the migration of the antiperiplanar carbon (C2) onto the oxime nitrogen. Closing up of the N1–C1–C2 bond angle, as with increasing electron demand of the OR group, reflects the increasing strength of the σ_{CC}–σ^*_{NOR} interaction due to the improved energy match between the σ_{CC} bonding orbital and the -σ^*_{NOR} antibonding orbital. The relationship between the N1–C1–C2 bond angle and pK_a for ROH which is represented by Eqn 3, shows more scatter than Eqn 2, and likely reflects the greater susceptibility of bond angles to variation as a result of differing packing effects associated with each structure.

$$\text{N1–C1–C2}\ [^\circ] = 114.8 + (1.5 \times 10^{-1})\ \text{p}K_a\ (\text{ROH}) + 114.86 \quad R^2 = 0.67 \tag{3}$$

*Structural Effects in 2,2-Dimethylcyclohexanone Oxime Derivatives **5a**–**5h***

A plot of N–OR bond distance vs pK_a (ROH) for the 2,2-dimethylcyclohexanone oxime derivatives **5a**–**5h** is presented in Fig. 6, and also establishes a clear relationship between the N–OR bond distance and the electron demand of the OR group (Eqn 4). However when compared to the cyclohexanone oxime derivatives **1a**–**1l** the response of the N–OR bond distance to the pK_a (ROH) is weaker:

$$\mathbf{5}\text{: } r_{N\text{–}OR}\ [\text{Å}] = 1.467 - (3.20 \times 10^{3})\ \text{p}K_a\ (\text{ROH}) \quad R^2 = 0.95 \tag{4}$$

Table 3. Selected bond angles [°] and dihedral angles [°] for derivatives of oximes 1a, 4a, and 5a

	O1–N1–C1	N1–C1–C2	N1–C1–C6	C2–C1–C6	C2–C1–N1–O1	C6–C1–N1–O1
1a	113.4(1)	117.5(2)	125.8(1)	116.7(1)	177.0(2)	1.9(2)
1b	112.7(1)	116.1(1)	128.3(1)	115.5(1)	176.3(1)	−1.2(2)
1c	108.9(1)	115.1(1)	128.8(1)	116.0(1)	179.6(2)	2.1(2)
1d	109.7(1)	114.8(2)	129.0(2)	116.2(2)	174.1(2)	5.2(2)
1g	108.7(1)	115.6(1)	128.9(1)	115.5(1)	176.7(1)	−2.9(2)
1h	109.4(2)	114.0(2)	130.0(2)	115.9(2)	177.3(2)	1.8(3)
1i	109.1(1)	115.0(1)	127.7(1)	117.3(1)	178.1(1)	−1.2(2)
1j	109.8(4)	115.2(4)	127.5(4)	117.3(4)	177.8(4)	−3.3(7)
4b	109.0(1)	116.1(2)	129.3(2)	114.1(2)	−177.0(2)	−1.2(3)
4d	109.7(1)	115.0(1)	129.3(1)	115.9(1)	178.5(1)	0.0(2)
4g	108.6(1)	115.7(1)	129.1(1)	115.0(1)	177.1(1)	1.8(2)
5a	113.5(1)	117.4(2)	125.3(2)	117.3(1)	178.5(2)	2.2(2)
5b	110.2(1)	116.1(1)	126.3(1)	117.6(1)	175.9(2)	−2.5(2)
5c	108.7(1)	116.7(1)	129.1(1)	116.2(1)	178.1(1)	0.0(2)
5e	109.0(1)	116.0(1)	126.7(1)	117.2(1)	−173.0(1)	6.1(2)
5f	109.54(9)	114.8(1)	127.5(1)	117.66(9)	−179.64(8)	−1.2(2)
5h	110.5(2)	115.6(2)	127.7(2)	116.7(2)	176.6(2)	−3.0(2)
8	111.7(1)	116.1(1)	127.6(1)	116.2(1)	179.1(2)	1.2(2)
9	109.3(1)	115.7(1)	128.4(1)	115.8(1)	179.9(2)	−2.2(2)

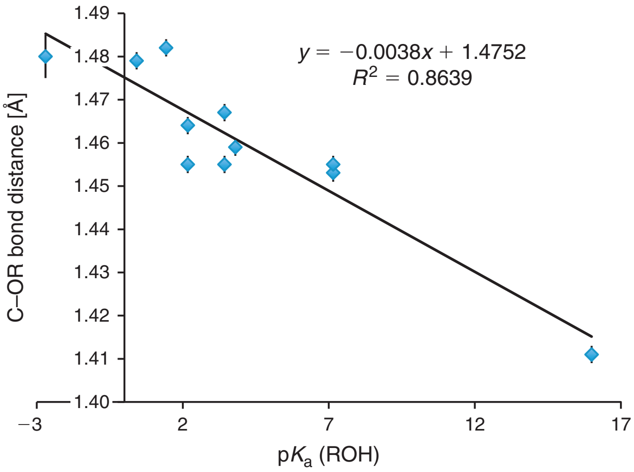

Fig. 3. Plot of C–OR bond distance vs pK_a (ROH) for cyclohexanone oxime derivatives (**1a**–**1j**, **8**, **9**).

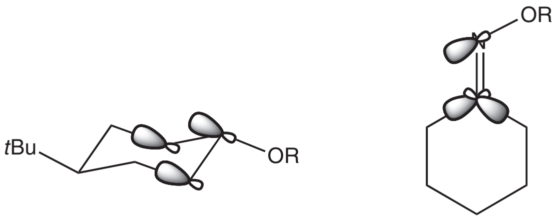

10 **1**

Fig. 4. Application of the variable oxygen probe: comparison between σ_{CC}–σ^*_{CO} interactions in derivatives of cyclohexanol **10** and σ_{CC}–σ^*_{NO} interactions in the oxime derivatives **1**.

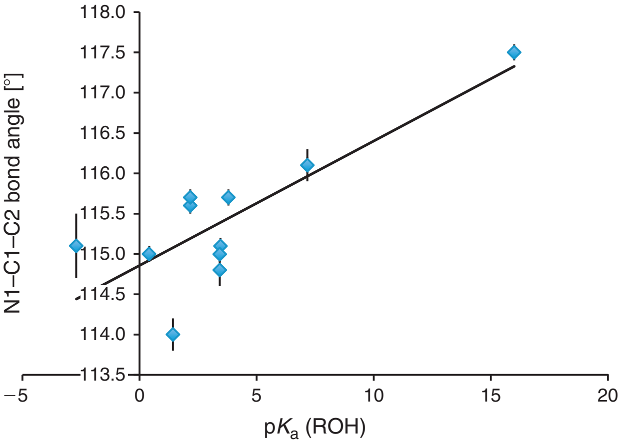

Fig. 5. Plot of the N1–C1–C2 bond angle [°] vs pK_a (ROH) for oxime derivatives (**1a**–**1j**, **4b**–**4g**, and **8**, **9**).

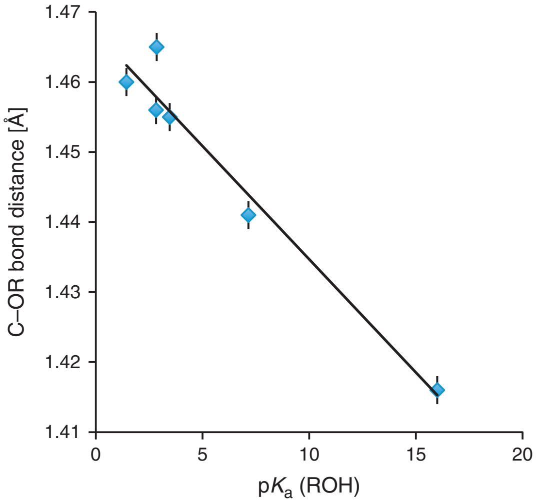

Fig. 6. Plot of C–OR bond distance vs pK_a (ROH) for cyclohexanone oxime derivatives (**5a**–**5h**).

Plotting the N1–C1–C2 bond angle as a function of the electron demand of the –OR substituent for the derivatives **5a**–**5h** gives rise to the relationship shown in Fig. 7. This demonstrates that the bond angle also closes up with increasing electron demand, however the response of the N1–C1–C2 bond

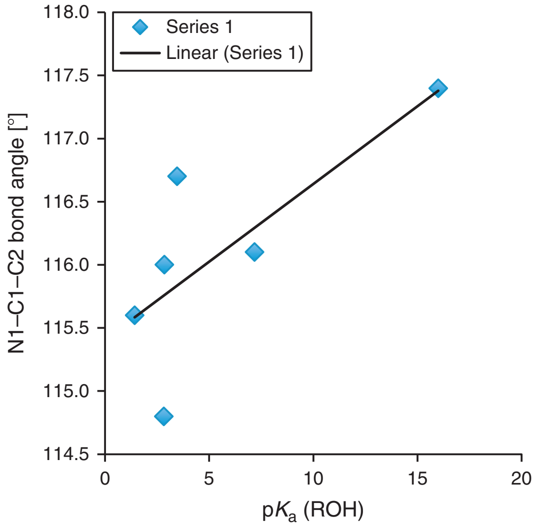

Fig. 7. Plot of the N1–C2–C2 bond angle [°] vs pK_a (ROH) for cyclohexanone oxime derivatives (**5a**–**5h**).

angle to the electron demand of the OR group in **5a**–**5h** is weaker than that observed for the cyclohexanone oxime derivatives **1a**–**1j**, **4b**–**4g**, and **8**–**9**. Although a smaller variation of the N1–C1–C2 bond angle in **5a**–**5h** might be expected, since closing up of this angle would be hindered due to steric interactions between the gem-dimethyl substituents with the oxime nitrogen, the poor correlation coefficient (Eqn 5) limits the conclusions that can be made based on this data.

$$\mathrm{N1{-}C1{-}C2}\ [^\circ] = 115.4 + (1.2 \times 10^{-1})\ \mathrm{p}K_a\ (\mathrm{ROH}) + 114.86 \quad R^2 = 0.56 \tag{5}$$

Effects of Varying Electron Demand of (OR) on the Carbon–Carbon Bond Distances

Examination of the bond distances in Table 2 shows that in the simple cyclohexanone oxime derivatives **1a**–**h**, **4b**, **4d**, **4g**, **8**, and **9** there is little difference between the antiperiplanar and synperiplanar C–C bond distances, although in all but one case, the antiperiplanar bond is slightly longer. For the 2,2-dimethylcyclohexanone oxime derivatives **5a**–**5h** the antiperiplanar C–C bond is on average 0.015 Å longer than the synperiplanar C–C bond. This is to be expected due to the differing extents of substitution of these two carbon–carbon bonds. Unfortunately, any effects on the carbon–carbon bond distances with varying electron demand of the OR substituent are not observable using X-ray crystallography. The effects are either too small to be reliably measured by this technique, and/or the measured carbon–carbon bond distances are too sensitive to other effects such as crystal packing and thermal libration effects, which may differ from structure to structure. Thus it was decided to look at trends of the ^{13}C–^{13}C one-bond coupling constants in these oxime derivatives as a function of the electron demand of the OR substituent. It has been demonstrated that there is a correlation between carbon–carbon bond distances and the corresponding ^{13}C–^{13}C 1-bond coupling constant, provided the carbon–carbon bonds being compared are similar with respect to substitution.[27] Vogel also showed that ^{13}C–^{13}C one-bond coupling constants are sensitive to the effects of hyperconjugation,[28] which was considered relevant to this study. The ^{13}C–^{13}C 1-bond coupling constants were determined for the oxime derivatives **1a**–**1g** and **4a**–**4h** using the 1D INADEQUATE pulse sequence.[28] The ^{13}C–^{13}C coupling constants for the antiperiplanar carbon–carbon bond and the synperiplanar carbon–carbon bond for **1a**–**1g** and **4a**–**4h** are presented in Table 4. The assignment of these carbons is clear and unambiguous, and has been reported before for the parent oxime **1a**.

Table 4. ^1J (^{13}C–^{13}C) coupling constants for the oxime derivatives 1a–1i and 4a–4i
All spectra recorded in CDCl$_3$ at 298 K. Coupling constant [Hz] values are ±0.2 Hz

	^1J (C1–C2) [Hz]	^1J (C1–C6) [Hz]
1a	46.2	38.6
1b	44.4	37.6
1c	43.3	37.9
1d	43.4	37.6
1e	43.4	38.5
1f	43.0	38.8
1g	42.6	37.9
1h	42.6	38.0
1i	42.3	37.6
4a	46.2	38.6
4b	44.4	37.6
4c	43.3	37.9
4d	43.4	37.6
4e	43.1	37.5
4f	43.1	37.7
4g	42.9	37.9
4h	42.9	37.6
4i	42.7	37.5

Inspection of the data contained in Table 3 show that the one-bond ^{13}C–^{13}C coupling constant for C1–C2 (the antiperiplanar carbon–carbon bond) is approximately 6 Hz larger than the synperiplanar carbon–carbon bond (C1–C6). This is a feature of oximes that has been noted previously[29] and has been used in many cases to assign stereochemistry to oxime derivatives.[30] The origin of this difference has been suggested to arise from a n_N–σ^*_{C-C} interaction between the oxime nitrogen lone pair electrons and the *syn* carbon–carbon antibonding orbital (e.g. structure **11** as depicted in Fig. 8),[29d] which is essentially an anomeric effect. Interestingly, in the protonated oxime derivative **12**, the *anti* and *syn* carbon–carbon coupling constants become very similar; however, the fact that the coupling constant for the *anti* carbon–carbon bond decreases upon protonation, rather than the *syn* carbon–carbon coupling constant increasing, suggests that the nitrogen lone pair makes a positive contribution to the coupling constant of the *anti* carbon–carbon bond, rather than decreasing the *syn* carbon–carbon coupling constant. This suggests that n_N–σ^*_{C-C} delocalisation is not the sole reason for this behaviour, but rather it is the result of several factors which have been discussed in the literature.[30]

The data in Table 3 can be used to construct plots of ^{13}C–^{13}C coupling constants for the *anti* and *syn* carbon–carbon bonds vs the electron demand of the –OR substituent as quantified by pK_a (ROH). These plots are presented in Figs 9 and 10 respectively. The *anti* ^{13}C–^{13}C coupling constants (Fig. 9) show a strong and well defined trend with varying electron demand of the oxygenated leaving group. The coupling constant clearly decreases with increasing electron demand of the leaving group.

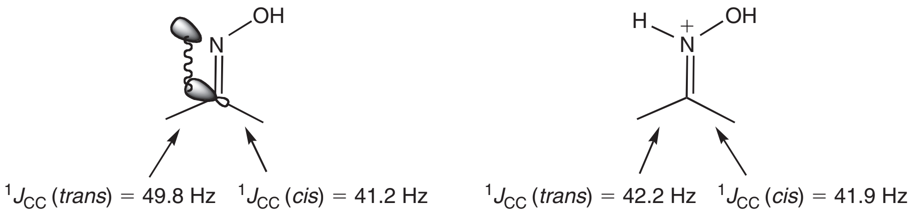

11 **12**

Fig. 8. ^1J (^{13}C–^{13}C) coupling constants for acetone oxime **11** and its protonated derivative **12**.

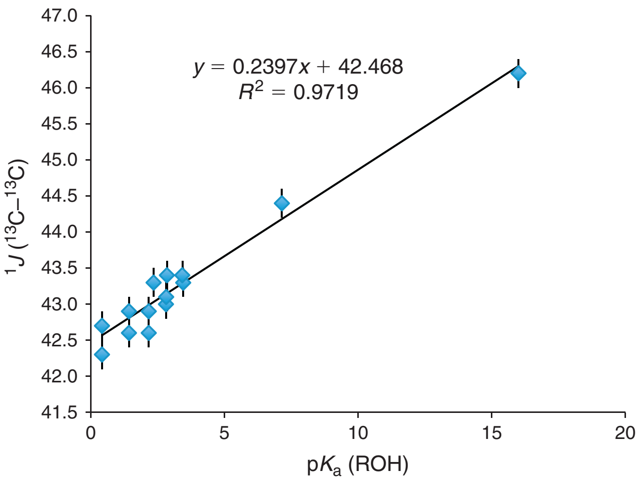

Fig. 9. Plot of ^1J (^{13}C–^{13}C) for the antiperiplanar bond (C1–C2) vs pK_a (ROH) for oxime derivatives **1a**–**1i**, and **4a**–**4i**.

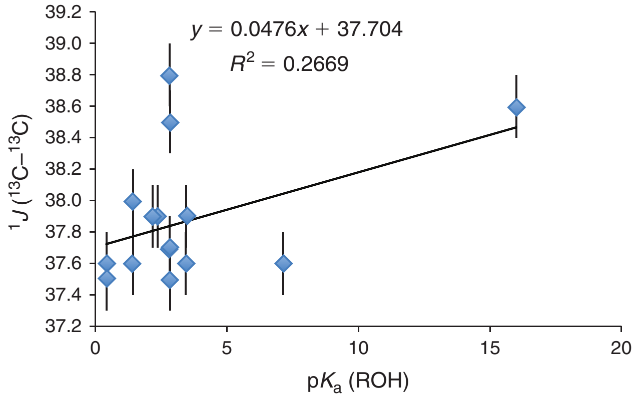

Fig. 10. Plot of ^1J (^{13}C–^{13}C) for the synperiplanar bond (C1–C6) vs pK_a (ROH) for oxime derivatives **1a**–**1i**, and **4a**–**4i**.

This is consistent with the expected bond weakening effects of the $\sigma_{C\text{–}C}$–$\sigma^*_{N\text{–}O}$ hyperconjugative interaction between the *anti* carbon–carbon bond and the N–OR antibonding orbital. Thus as the electron demand of the OR group increases, the energy of the N–OR antibonding orbital decreases and becomes a better acceptor; this results in a stronger interaction with the *anti* carbon–carbon bond. As a result of the stronger $\sigma_{C\text{–}C}$–$\sigma^*_{N\text{–}O}$ interaction, the *anti* ^{13}C–^{13}C bond is weakened, and hence the coupling constant decreases.

The plot can be used to generate the following equation (Eqn 6), which relates the coupling constant of the *anti* carbon–carbon bond (C1–C2) to the electron demand of the oxygen substituent as quantified by the pK_a value for its parent acid (ROH):

$$^1J\ (^{13}\mathrm{C}\text{–}^{13}\mathrm{C})\ [\mathrm{Hz}] = 42.452 + (2.25 \times 10^{-1})\ \mathrm{p}K_a\ (\mathrm{ROH}) \qquad R^2 = 0.972 \qquad (6)$$

Examination of the plot of the coupling constant for the *syn* carbon–carbon bond (C1–C6) with electron demand of the oxygen substituent (Fig. 10) shows that this coupling constant appears to vary in a similar way as the *anti* coupling constant such that as the electron demand of the oxygen substituent increases, the *syn* (C1–C6) coupling constant decreases. However, the trend is poorly defined with a weaker correlation being apparent. The larger scatter in the coupling constant data for the *syn* carbon–carbon bond (C1–C6) may be due to the fact that the oxygenated substituent (OR) not only exerts an electronic effect on this bond, but due to its close proximity, it may also exert a varying steric effect. The trend line in Fig. 10 is represented Eqn 7:

$$^1J\ (^{13}\mathrm{C}\text{–}^{13}\mathrm{C})\ [\mathrm{Hz}] = 37.651 + (7.90 \times 10^{-2})\ \mathrm{p}K_a\ (\mathrm{ROH}) \qquad R^2 = 0.22 \qquad (7)$$

Comparison with Eqn 6 derived for the *anti* carbon–carbon bond reveals that the coupling constant for the *anti* bond (C1–C2) is at least three times more sensitive to the electron demand of the oxygen substituent than the coupling constant for the *syn* bond (C1–C6). This result is consistent with the expected effects of the $\sigma_{C\text{–}C}$–$\sigma^*_{N\text{–}O}$ interaction for both the *anti* (C1–C2) and *syn* (C1–C6) bonds. The *anti* bond (C1–C2) has more effective overlap with the N–OR antibonding orbital than the *syn* bond (C1–C6), therefore the bond strength and the coupling constant should be more sensitive to the electron demand of the OR substituent.

Conclusion

X-ray structural data of cyclohexanone oximes and their derivatives were analysed. These data, which expand upon the early reports by Kirby et al.[15] show that as the electron demand of the OR group increases, then the early stages of the Beckmann rearrangement become clear; the increase of N–OR bond distance shows the early stages of the heterolysis of this bond, and the closing up of C2–C1–N bond angle as the *anti* carbon (C2) begins to migrate onto the oxime nitrogen. Trends of the *anti* and *syn* carbon–carbon bond distances with increasing electron demand of the OR group, which might reflect increasing σ_{CC}–σ^*_{NO} hyperconjugation, were however not apparent from the structural data, although the *anti* bond (C2–C1) was consistently longer than the *syn* bond (C1–C6) in all structures. Evidence for participation of the *anti* carbon–carbon bond in the early stages of the Beckmann rearrangement was provided by analysis of the one-bond ^{13}C–^{13}C coupling constants in the derivatives **1a**–**1i** and **4a**–**4l** as a function of the electron demand of the OR substituent. The structural effects in the oxime derivatives **5a**–**5c**, **5e**, **5f**, and **5h** of 2,2-dimethylcyclohexanone, which undergoes Beckmann fragmentation, were similar to those observed in the simple cyclohexanone derivatives, but were smaller in magnitude.

Supplementary Material

Crystallographic information files for **1b**–**1d**, **1g**–**1j**, **4b**, **4d**, **4g**, **5a**–**5c**, **5e**, **5f**, and **5h** have been deposited with the Cambridge Crystallographic Data Centre and assigned CCDC codes 870259–870263 respectively.

Experimental

Crystallography

Crystallographic diffraction data were collected with either a Bruker SMART Apex CCD detector using Mo Kα radiation ($\lambda = 0.71073$ Å), or an Oxford Diffraction Sapphire CCD diffractometer using Cu-Ka radiation (graphite crystal monochromator ($\lambda = 1.54184$ Å), or on an Oxford SuperNova diffractometer using Cu or Mo radiation. Data collected on the Bruker diffractometer were reduced using the program SAINT[2] while data collected on the Oxford diffractometer were reduced using the CrysalisPRO software. The temperature of the data collections were maintained at 130 K, using an Oxford Cryostream cooling device. The structures were solved by direct methods, differences Fourier synthesis, and were refined on F^2 (SHELXL-97).[31] Thermal ellipsoid plots were generated using the program ORTEP-3[32] integrated within the WINGX program suite.[33]

Crystal Data for 1b

$C_{12}H_{14}N_2O_3$, $M = 234.25$, $T = 130.0(2)$ K, $\lambda = 1.5418$, monoclinic, space group P2$_1$/c, $a = 6.9400(1)$, $b = 16.1184(4)$, $c = 10.4188(2)$ Å, $\beta = 104.618(2)°$, $V = 1127.74(4)$ Å^3, $Z = 4$, $D_c = 1.380$ Mg M^{-3}, μ(Cu-Kα) 0.832 mm^{-1}, $F(000) = 496$, crystal size 0.72 × 0.45 × 0.18 mm. 3656 Reflections measured, 1708 independent reflections ($R_{int} = 0.028$), the final R was 0.0385 [$I > 2\sigma(I)$], and $wR(F^2)$ was 0.1132 (all data).

Crystal Data for 1c

$C_{13}H_{14}N_2O_4$, $M = 262.26$, $T = 130.0(2)$ K, $\lambda = 0.71073$, monoclinic, space group P2$_1$/c, $a = 18.456(5)$, $b = 7.940(2)$, $c = 8.163(2)$ Å, $\beta = 96.298(5)°$, $V = 1189.0(6)$ Å^3, $Z = 4$, $D_c = 1.465$ Mg M^{-3}, μ(Mo-Kα) 0.110 mm^{-1}, $F(000) = 552$, crystal size 0.45 × 0.25 × 0.20 mm. 7157 Reflections measured, 2689 independent reflections ($R_{int} = 0.022$), the final R was 0.0427 [$I > 2\sigma(I)$], and $wR(F^2)$ was 0.1131 (all data).

Crystal Data for 1e

$C_{13}H_{13}N_3O_6$, $M = 307.26$, $T = 130.0(2)$ K, $\lambda = 0.71073$, orthorhombic, space group P2$_1$2$_1$2$_1$, $a = 6.3148(8)$, $b = 9.3102(12)$, $c = 23.318(3)$ Å, $V = 1370.9(3)$ Å^3, $Z = 4$, $D_c = 1.489$ Mg M^{-3} μ(Mo-Kα) 0.120 mm^{-1}, $F(000) = 640$, crystal size 0.40 × 0.40 × 0.07 mm. 7173 Reflections measured, 2410 independent reflections ($R_{int} = 0.059$), the final R was 0.0422 [$I > 2\sigma(I)$], and $wR(F^2)$ was 0.0899 (all data).

Crystal Data for 1g

$C_{13}H_{14}N_2O_4$, $M = 262.26$, $T = 130.0(2)$ K, $\lambda = 0.71073$, orthorhombic, space group Pna2$_1$, $a = 10.9742(8)$, $b = 9.7851(7)$, $c = 11.7102(9)$ Å, $V = 1257.48(16)$ Å^3, $Z = 4$, $D_c = 1.385$ Mg M^{-3} μ(Mo-Kα) 0.104 mm^{-1}, $F(000) = 552$, crystal size 0.25 × 0.20 × 0.10 mm. 7481 Reflections measured, 2628 independent reflections ($R_{int} = 0.044$), the final R was 0.0337 [$I > 2\sigma(I)$], and $wR(F^2)$ was 0.0795 (all data).

Crystal Data for 1h

$C_{13}H_{13}N_3O_6$, $M = 307.26$, $T = 130.0(2)$ K, $\lambda = 0.71073$ orthorhombic, space group Pccn, $a = 25.456(4)$, $b = 9.745(2)$, $c = 11.407(2)$ Å, $V = 1127.74(4)$ Å^3, $Z = 8$, $D_c = 1.442$ Mg M^{-3} μ(Mo-Kα) 0.116 mm^{-1}, $F(000) = 1280$, crystal size 0.45 × 0.40 × 0.30 mm. 13593 Reflections measured, 2497 independent reflections ($R_{int} = 0.11$), the final R was 0.0485 [$I > 2\sigma(I)$], and $wR(F^2)$ was 0.1232 (all data).

Crystal Data for 1i

$C_{12}H_{12}N_4O_7$, $M = 324.26$, $T = 130.0(2)$ K, $\lambda = 0.71073$ monoclinic, space group P2$_1$/c, $a = 10.693(5)$, $b = 12.549(5)$, $c = 10.792(5)$ Å, $\beta = 100.225(5)°$, $V = 1425.1(1)$ Å^3, $Z = 4$, $D_c = 1.511$ Mg M^{-3} μ(Mo-Kα) 0.127 mm^{-1}, $F(000) = 672$, crystal size 0.45 × 0.37 × 0.27 mm. 7745 Reflections measured, 2722 independent reflections ($R_{int} = 0.040$), the final R was 0.0392 [$I > 2\sigma(I)$], and $wR(F^2)$ was 0.1196 (all data).

Crystal Data for 1j

$C_{13}H_{17}NO_3S$, $M = 267.34$, $T = 130.0(2)$ K, $\lambda = 0.71073$ monoclinic, space group Cc, $a = 8.780(5)$, $b = 16.387(5)$, $c = 9.395(5)$ Å, $\beta = 103.956(5)°$, $V = 1311.8(11)$ Å^3, $Z = 4$, $D_c = 1.354$ Mg M^{-3} μ(Mo-Kα) 0.247 mm^{-1}, $F(000) = 568$, crystal size 0.60 × 0.14 × 0.06 mm. 3206 Reflections measured, 1701 independent reflections ($R_{int} = 0.035$), the final R was 0.0546 [$I > 2\sigma(I)$], and $wR(F^2)$ was 0.1545 (all data).

Crystal Data for 4b

$C_{16}H_{22}N_2O_3$, $M = 290.36$, $T = 130.0(2)$ K, $\lambda = 0.71073$ monoclinic, space group P2$_1$/n, $a = 5.894(1)$, $b = 21.236(5)$, $c = 12.081(3)$ Å, $\beta = 91.271(4)°$, $V = 1511.8(6)$ Å^3, $Z = 4$, $D_c = 1.276$ Mg M^{-3} μ(Mo-Kα) 0.088 mm^{-1}, $F(000) = 624$, crystal size 0.50 × 0.45 × 0.35 mm. 7547 Reflections measured, 2622 independent reflections ($R_{int} = 0.035$), the final R was 0.0492 [$I > 2\sigma(I)$], and $wR(F^2)$ was 0.1290 (all data).

Crystal Data for 4d

$C_{17}H_{22}N_2O_4$, $M = 318.37$, $T = 130.0(2)$ K, $\lambda = 0.71073$, orthorhombic, space group P2$_1$2$_1$2$_1$, $a = 6.4425(5)$, $b = 11.9620(9)$, $c = 21.5769(16)$ Å, $V = 1662.8(2)$ Å^3, $Z = 4$, $D_c = 1.272$ Mg M^{-3} μ(Mo-Kα) 0.091 mm^{-1}, $F(000) = 680$, crystal size 0.50 × 0.40 × 0.30 mm. 8812 Reflections measured, 2927 independent reflections ($R_{int} = 0.047$), the final R was 0.0321 [$I > 2\sigma(I)$], and $wR(F^2)$ was 0.0703 (all data).

Crystal Data for 4g

$C_{17}H_{22}N_2O_4$, $M = 318.37$, $T = 130.0(2)$ K, $\lambda = 1.54184$ Å monoclinic, space group P2$_1$/n, $a = 9.3991(1)$, $b = 15.2220(1)$,

$c = 12.5030(1)$ Å, $\beta = 109.367(1)°$, $V = 1687.62(3)$ Å^3, $Z = 4$, $D_c = 1.253$ Mg M^{-3} μ(Cu-Kα) 0.736 mm^{-1}, $F(000) = 680$, crystal size 0.60 × 0.46 × 0.30 mm. 8395 Reflections measured, 3313 independent reflections ($R_{int} = 0.035$), the final R was 0.0385 [$I > 2\sigma(I)$], and $wR(F^2)$ was 0.1057 (all data).

Crystal Data for **5a**

$C_8H_{15}NO$, $M = 141.21$, $T = 130.0(2)$ K, $\lambda = 1.54184$, monoclinic, space group P2$_1$/n $a = 7.7390(7)$, $b = 10.1658(8)$, $c = 11.1940(8)$ Å, $\beta = 108.213(9)°$, $V = 836.55(12)$ Å^3, $Z = 4$, $D_c = 1.121$ Mg M^{-3} μ(Cu-Kα) 0.577 mm^{-1}, $F(000) = 312$, crystal size 0.30 × 0.26 × 0.03 mm. 2991 Reflections measured, 1503 independent reflections ($R_{int} = 0.028$), the final R was 0.0446 [$I > 2\sigma(I)$], and $wR(F^2)$ was 0.1152 (all data).

Crystal Data for **5b**

$C_{14}H_{18}N_2O_3$, $M = 262.30$, $T = 130.0(2)$ K, $\lambda = 1.5418$, triclinic, space group P-1 $a = 7.0117(5)$, $b = 7.3439(5)$, $c = 14.553(1)$ Å, $\alpha = 76.064(6)°$, $\beta = 87.672(6)°$, $\gamma = 69.413(7)°$, $V = 680.06(8)$ Å^3, $Z = 2$, $D_c = 1.281$ Mg M^{-3} μ(Cu-Kα) 0.744 mm^{-1}, $F(000) = 280$, crystal size 0.32 × 0.27 × 0.06 mm. 3704 Reflections measured, 2412 independent reflections ($R_{int} = 0.019$), the final R was 0.0396 [$I > 2\sigma(I)$], and $wR(F^2)$ was 0.1178 (all data).

Crystal Data for **5c**

$C_{15}H_{18}N_2O_4$, $M = 290.31$, $T = 130.0(2)$ K, $\lambda = 1.5418$, monoclinic, space group P2$_1$/c $a = 11.3138(2)$, $b = 12.9150(2)$, $c = 10.7704(2)$ Å, $\beta = 110.951(2)°$, $V = 1469.70(4)$ Å^3, $Z = 4$, $D_c = 1.312$ Mg M^{-3} μ(Cu-Kα) 0.795 mm^{-1}, $F(000) = 616$, crystal size 0.38 × 0.35 × 0.26 mm. 5173 Reflections measured, 2643 independent reflections ($R_{int} = 0.014$), the final R was 0.0376 [$I > 2\sigma(I)$], and $wR(F^2)$ was 0.1048 (all data).

Crystal Data for **5e**

$C_{15}H_{17}N_3O_6$, $M = 335.32$, $T = 130.0(2)$ K, $\lambda = 1.54184$, orthorhombic, space group Pccn, $a = 27.8924(6)$, $b = 11.7985(3)$, $c = 9.8731(2)$ Å, $V = 3249.1(1)$ Å^3, $Z = 8$, $D_c = 1.371$ Mg M^{-3} μ(Cu-Kα) 0.912 mm^{-1}, $F(000) = 1408$, crystal size 0.40 × 0.26 × 0.09 mm. 7040 Reflections measured, 2928 independent reflections ($R_{int} = 0.020$), the final R was 0.0405 [$I > 2\sigma(I)$], and $wR(F^2)$ was 0.1193 (all data).

Crystal Data for **5f**

$C_{15}H_{17}N_3O_6$, $M = 335.32$, $T = 130.0(2)$ K, $\lambda = 1.54184$, monoclinic, space group P2$_1$/n, $a = 11.9121(7)$, $b = 7.7814(2)$, $c = 9.3550(2)$ Å, $\beta = 100.101(5)°$, $V = 1601.64(13)$ Å^3, $Z = 4$, $D_c = 1.391$ Mg M^{-3} μ(Cu-Kα) 0.925 mm^{-1}, $F(000) = 704$, crystal size 0.48 × 0.30 × 0.18 mm. 10999 Reflections measured, 3207 independent reflections ($R_{int} = 0.018$), the final R was 0.0345 [$I > 2\sigma(I)$], and $wR(F^2)$ was 0.0935 (all data).

Crystal Data for **5h**

$C_{15}H_{17}N_3O_6$, $M = 335.32$, $T = 130.0(2)$ K, $\lambda = 1.54184$, monoclinic, space group P2$_1$, $a = 7.7384(1)$, $b = 10.8085(2)$, $c = 9.3550(2)$ Å, $\beta = 90.465(2)°$, $V = 782.43(2)$ Å^3, $Z = 2$, $D_c = 1.423$ Mg M^{-3} μ(Cu-Kα) 0.946 mm^{-1}, $F(000) = 352$, crystal size 0.20 × 0.16 × 0.014 mm. 2648 Reflections measured, 2056 independent reflections ($R_{int} = 0.026$), the final R was 0.0325 [$I > 2\sigma(I)$], and $wR(F^2)$ was 0.0768 (all data).

Synthesis

General experimental details have been published elsewhere.[11f]

Cyclohexanone O-4-Nitrophenyl Oxime (**1b**)

Potassium hydride (74.1 mg, 1.85 mmol) was added to a solution of oxime **1a** (209 mg, 1.85 mmol) in THF (15 mL). 4-Fluoronitrobenzene (261 mg, 0.20 mL, 1.85 mmol) was then added to this mixture and the reaction stirred for 2 h. The reaction was quenched by the addition of water, then extracted into ether (50 mL). The ether layer was washed with water, dried ($MgSO_4$) and evaporated under reduced pressure to give *p*-nitrophenoxy derivative **1b** which was purified by flash column chromatography (Et_2O/light petroleum) to give a light yellow solid (124 mg, 21 %), which was recrystallised from dichloromethane to give colourless blocks, mp = 96.8–97.6°C. ^{1}H NMR: δ 8.14 (2H, d, $J = 9.2$ Hz), 7.21 (2H, d, $J = 9.2$ Hz), 2.63 (2H, t, $J = 6.2$ Hz), 2.34 (2H, t, $J = 6.2$ Hz), 1.75–1.62 (6H, m), ^{13}C NMR: δ 166.20, 164.34, 141.93, 125.67, 114.14, 32.01, 26.97, 26.28, 25.82, 25.53, IR ν_{max}: 3117, 3071, 3016, 2934, 2856, 164, 1604, 1506, 1485, 1335, 886 cm^{-1}. HRMS (ESI): Calcd $C_{12}H_{14}N_2O_3$ [M+Na]$^+$ 235.10772, found [M+Na]$^+$ 235.10773.

Cyclohexanone O-3-Nitrobenzoyl Oxime (**1c**)

Standard procedure for preparation of O-acyl oxime derivatives. Oxime **1a** (0.4 g, 3.53 mmol) in dichloromethane (8 mL) and pyridine (2 mL) was treated with 3-nitrobenzoyl chloride (689 mg, 3.71 mmol), and stirred for 10 h under an atmosphere of nitrogen. The reaction was quenched by the addition of water, and the resulting mixture diluted with dichloromethane (30 mL) followed by washing with 10 % aqueous $NaHCO_3$ (2 × 20 mL), water (1 × 20 mL), then saturated $CuSO_4$ solution (3 × 20 mL). The solvent was dried ($MgSO_4$) and evaporated under reduced pressure (to afford product **1c** as a beige solid (846 mg, 91 %), which was recrystallised from dichloromethane to give beige blocks, mp = 109.6–110.7°C. ^{1}H NMR: δ 8.84 (1H, s), 8.43 (1H, d, $J = 8.0$ Hz), 8.38 (1H, d, $J = 8.0$ Hz), 7.68 (1H, t, $J = 8.0$ Hz), 2.68 (2H, t, $J = 6.4$ Hz), 2.47 (2H, t, $J = 6.2$ Hz) 1.82 (4H, m), 1.66 (2H, m), ^{13}C NMR: δ 169.82, 161.30, 147.45, 134.38, 130.37, 129.33, 126.79, 123.45, 31.31, 26.43, 26.06, 25.15, 24.57. IR ν_{max}: 3100, 3086, 2990, 2971, 2937, 2866, 1742, 1638, 1618, 1533, 1440, 1366, 1348, 822 cm^{-1}. HRMS (ESI): Calcd $C_{13}H_{14}N_2O_4$ [M+Na]$^+$ 285.08458, found [M+Na]$^+$ 285.08465.

Cyclohexanone O-4-Nitrobenzoyl Oxime (**1d**)

Following the general procedure described above for the preparation of **1c**, oxime **1a** (0.5 g, 4.42 mmol) in dichloromethane (5 mL), THF (5 mL) and pyridine (5 mL) was treated with 4-nitrobenzoyl chloride (861 mg, 4.64 mmol) for 12 h to afford product **1d** as a pale yellow solid (1.0 g, 86 %), which was recrystallised from dichlromethane to give brown blocks, mp = 102.1–104.1°C. ^{1}H NMR: δ 8.29 (2H, d, $J = 7.2$ Hz), 8.21 (2H, d, $J = 7.2$ Hz), 2.66 (2H, t, $J = 6.3$ Hz), 2.46 (2H, t, $J = 6.3$ Hz), 1.75 (4H, m), 1.65 (2H, d, $J = 5.2$ Hz), ^{13}C NMR: δ 170.18, 161.91, 150.08, 134.45, 130.21, 123.18, 31.64, 26.78, 26.34, 25.45, 24.88, IR ν_{max}: 3017, 2970, 2949, 2854, 1737, 1631, 1608, 1525, 1447, 1426, 1366, 854 cm^{-1}. HRMS (ESI): Calcd $C_{13}H_{14}N_2O_4$ [M+Na]$^+$ 285.08458, found [M+Na]$^+$ 285.08467.

Cyclohexanone O-3,5-Dinitrobenzoyl Oxime (1e)

Following the general procedure oxime **1a** (0.4 g, 3.53 mmol) in dichloromethane (8 mL) and pyridine (3 mL) was treated with 3,5-dinitrobenzoyl chloride (856 mg, 3.71 mmol) for 12 h to afford product **1e** as a light brown solid (963 mg, 87 %), which was recrystallised from dichloromethane to give colourless blocks, mp = 114.8–115.0°C. ^{1}H NMR: δ 9.24 (1H, s), 9.16 (2H, s), 2.70 (2H, t, $J = 6.4$ Hz), 2.50 (2H, t, $J = 6.4$ Hz), 1.82 (4H, m), 1.71 (2H, m), ^{13}C NMR: δ 171.29, 160.07, 148.39, 132.87, 128.99, 122.22, 31.73, 27.08, 26.45, 25.61, 24.97, IR $\nu_{\max}$: 3104, 2943, 2885, 2858, 1752, 1631, 1598, 1541, 1459, 1447, 1347, 858 cm^{-1}. HRMS (ESI): Calcd $C_{13}H_{13}N_3O_6$ [M+Na]$^+$ 330.06966, found [M+Na]$^+$ 330.06979.

Cyclohexanone O-3,4-Dinitrobenzoyl Oxime (1f)

Following the general procedure, oxime **1a** (0.30 g, 2.65 mmol) in dichloromethane (7 mL) and pyridine (2 mL) was treated with 3,4-dinitrobenzoyl chloride (642 mg, 2.78 mmol) for 12 h to afford product **1f** as a brown solid (788 mg, 97 %), which was recrystallised from dichloromethane to give brown blocks, mp = 84.6–86.2°C. ^{1}H NMR: δ 8.53 (1H, d, $J = 1.7$ Hz,), 8.41 (1H, dd, $J = 8.4$, 1.7 Hz), 7.99 (1H, d, $J = 8.4$ Hz), 2.63 (2H, t, $J = 5.4$ Hz), 2.43 (2H, t, $J = 6.2$ Hz) 1.77 (4H, m), 1.65 (2H, d, $J = 4.4$ Hz), ^{13}C NMR: δ 171.11, 160.10, 144.64, 142.01, 134.26, 134.02, 131.96, 125.24, 31.12, 26.36, 26.16, 25.16, 24.48, IR $\nu_{\max}$: 3096, 2970, 2941, 2860, 1742, 1631, 1611, 1600, 1539, 1450, 1349, 845 cm^{-1}. HRMS (ESI): Calcd $C_{13}H_{13}N_3O_6$ [M+Na]$^+$ 330.06966, found [M+Na]$^+$ 330.06980.

Cyclohexanone O-2-Nitrobenzoyl Oxime (1g)

Following the general procedure, oxime **1b** (0.20 g, 1.77 mmol) in THF (5 mL) and pyridine (2 mL) was treated with 2-nitrobenzoyl chloride (344 mg, 1.86 mmol) for 12 h to afford product **1g** as a dark brown solid (413 mg, 89 %), which was recrystallised from dichloromethane to give dark brown blocks, mp = 73.9–75.4°C. ^{1}H NMR: δ 7.65 (1H, d, $J = 8.0$ Hz), 7.42 (3H, m), 2.16 (2H, d, $J = 6.0$ Hz), 2.03 (2H, d, $J = 6.0$ Hz) 1.4–1.27 (6H, m), ^{13}C NMR: δ 169.76, 162.92, 146.97, 132.74, 131.40, 129.15, 125.85, 123.15, 31.09, 26.15, 26.01, 25.01, 24.35, IR $\nu_{\max}$: 3097, 3075, 2938, 2861, 1750, 1636, 1607, 1577, 1531, 1442, 1354, 855 cm^{-1}. HRMS (ESI): Calcd $C_{13}H_{14}N_2O_4$ [M+Na]$^+$ 285.08458, found [M+Na]$^+$ 285.08463.

Cyclohexanone O-2,4-Dinitrobenzoyl Oxime (1h)

Following the general procedure, oxime **1a** (189 mg, 1.67 mmol) in dichloromethane (5 mL) and pyridine (2 mL) was treated with 2,4-dinitrobenzoyl chloride (404 mg, 1.75 mmol) for 18 h to afford product **1h** as brown solid (418 mg, 81 %), which was recrystallised from dichloromethane to give brown plates, mp = 48.4–49.0°C. ^{1}H NMR: δ 8.71 (1H, d, J = 2.1 Hz), 8.55 (1H, dd, J = 8.2, 2.1 Hz), 7.9 (1H, d, J = 8.2 Hz), 2.44 (2H, bs), 2.25 (2H, bs), 1.05–1.03 (6H, m), ^{13}C NMR: δ 170.57, 161.92, 148.17, 146.74, 131.65, 130.80, 127.56, 118.74, 31.03, 26.28, 26.10, 25.10, 24.42. IR $\nu_{\max}$: 3111, 3090, 3059, 2961, 2933, 2860, 1742, 1636, 1604, 1543, 1531, 1446, 1358, 1349, 827 cm^{-1}. HRMS (ESI): Calcd $C_{13}H_{13}N_3O_6$ [M+Na]$^+$ 330.06966, found [M+Na]$^+$ 330.06975.

Cyclohexanone O-2,4,6-Trinitrophenyl Oxime (1i)

Oxime **1a** (1.0 g, 8.84 mmol) in dichloromethane (10 mL) was treated with triethylamine (1.85 mL, 1.34 g, 13.3 mmol) and 2,4,6-trinitrofluorobenzene (2.25 g, 9.72 mmol) to afford product **1i** as brown solid (1.78 g, 62 %), which was recrystallised from dichloromethane to give yellow blocks, mp = 104.4–105.1°C. ^{1}H NMR: δ 8.71 (2H, s), 2.60 (2H, t, $J = 6.2$ Hz), 2.18 (2H, t, $J = 6.2$ Hz), 1.70 (4H, m), 1.61 (2H, d, $J = 4.4$ Hz), ^{13}C NMR: δ 170.18, 150.30, 141.31, 139.96, 123.58, 30.56, 26.57, 25.38, 24.83, IR $\nu_{\max}$: 3096, 2944, 2863, 1672, 1611, 1539, 1343, 905 cm^{-1}. HRMS (ESI): Calcd $C_{12}H_{12}N_4O_7$ [M+Na]$^+$ 347.05982, found [M+Na]$^+$ 347.05984.

Cyclohexanone O-4-Toluenesulfonyl Oxime (1j)

4-Toluenesulfonyl chloride (2.53 g, 13.3 mmol) was added to oxime **1a** (1.5 g, 13.3 mmol) in pyridine over 20 min. The resultant mixture was stirred at −20°C for 3 h, then poured onto ice (50 g). The white murky mixture was filtered, washed thoroughly with water and dried to give compound **1j** as a white waxy solid (1.24 g, 35 %). Crystallization from toluene gave the Beckmann rearrangement product **6** as colourless plates, mp = 79.5–82.0°C. ^{1}H NMR: δ 10.21 (1H, bs), 9.62 (1H, bs), 7.67 (2H, d, $J = 7.8$ Hz), 7.13 (2H, d, $J = 7.8$ Hz, 3.34 (2H, bs), 2.62 (2H, bs), 2.29 (3H, s), 1.71 (2H, bs), 1.58 (4H, m), ^{13}C NMR: δ 182.50, 149.80, 140.48, 128.83, 125.66, 43.78, 32.86, 29.47, 26.64, 21.74, 21.12, IR $\nu_{\max}$: 3324, 3069, 2946, 2864, 1653, 1495, 1118, 682 cm^{-1}.

Crystallisation of the crude **1j** from dichloromethane in a dessicator containing P_2O_5 at −10°C gave **1j** as colourless plates, mp = 101.5–102.8°C. ^{1}H NMR: δ 8.14 (2H, d, $J = 9.2$ Hz), 7.21 (2H, d, $J = 9.2$ Hz), 2.63 (2H, t, $J = 6.2$ Hz), 2.34 (2H, t, $J = 6.2$ Hz), 1.75–1.62 (6H, m), ^{13}C NMR: δ 169.80, 144.61, 132.95, 129.44, 128.65, 31.67, 26.67, 26.53, 25.49, 25.06, 21.61, IR $\nu_{\max}$: 3099, 3060, 2993, 2945, 2867, 1648, 1597, 1443, 1362, 1180, 1172, 757 cm^{-1}. HRMS (ESI): Calcd $C_{13}H_{17}NO_3S$ [M+H]$^+$ 268.10019, found [M+H]$^+$ 268.10019.

4-tert-Butyl cyclohexanone O-4-Nitrophenyl Oxime (4b)

Following the general procedure employed for the preparation of **1b**, potassium hydride (23.7 mg, 59.1 mmol) was added to oxime **4a** (100 mg, 0.591 mmol) in THF (15 mL). 4-Fluoronitrobenzene (83.4 mg, 0.063 mL, 5.91 mmol) was then added to this mixture and stirred for 2 h giving **4b** as a light yellow solid (125 mg, 73 %), mp = 103.4–105.1°C, ^{1}H NMR: δ 8.17 (2H, d, $J = 9.2$ Hz), 7.24 (2H, d, $J = 9.2$ Hz), 3.46 (1H, d, $J = 12.4$ Hz), 2.60 (1H, dd, $J = 13.6$, 2.6 Hz), 2.06–1.93 (3H, m), 1.31–1.23 (4H, m), 0.88 (9H, m), ^{13}C NMR: δ 166.20, 164.30, 141.82, 125.58, 114.07, 47.20, 32.39, 31.73, 27.60, 27.43, 26.52, 26.00, IR $\nu_{\max}$: 3055, 3000, 2970, 1655, 1639, 1506, 1366, 1354, 880 cm^{-1}. HRMS (ESI): Calcd $C_{16}H_{23}N_2O_3$ [M+H]$^+$ 291.17032, found [M+H]$^+$ 291.17035.

4-tert-Butyl Cyclohexanone O-3-Nitrobenzoyl Oxime (4c)

Following general procedure, oxime **4a** (0.50 g, 2.95 mmol) in dichloromethane (7 mL) and pyridine (2 mL) was treated with 3-nitrobenzoyl chloride (576 mg, 3.10 mmol) for 10 h to afford product **4c** as a beige solid (676 mg, 72 %), mp = 109.7–111.0°C. ^{1}H NMR: δ 8.57 (1H, bs), 8.20 (1H, dd, $J = 7.9$, 2.2 Hz), 8.17 (1H, d, $J = 7.9$ Hz), 7.53 (1H, dd $J = 7.9$, 7.9 Hz,), 3.21 (1H, d, $J = 15.0$ Hz), 2.52 (1H, d, $J = 13.5$ Hz), 2.08–2.01 (1H, m), 1.85 (3H, m), 1.18–1.05 (3H, m), 0.67 (9H, s), ^{13}C NMR: δ 170.13, 161.59, 147.72, 134.65, 130.62, 129.47, 127.02, 123.73, 46.48, 31.89, 31.32, 26.97, 26.94, 26.51, 26.12, IR ν_{max}: 3099, 2961, 2866, 1742, 1638, 1615, 1528, 1440, 1367, 1343, 879 cm^{-1}. HRMS (ESI): Calcd $C_{17}H_{22}N_2O_4$ $[M+Na]^+$ 341.14718, found $[M+Na]^+$ 341.14733.

*4-tert-Butyl Cyclohexanone O-4-Nitrobenzoyl Oxime (**4d**)*

Following general procedure, oxime **4a** (0.50 g, 2.95 mmol) in dichloromethane (7 mL) and pyridine (2 mL) was treated with 4-nitrobenzoyl chloride (576 mg, 3.10 mmol) for 13 h to afford product **4d** as a beige solid (719 mg, 77 %), which was recrystallised from acetonitrile to give beige blocks, mp = 109.9–111.8°C. ^1H NMR: δ 8.29 (2H, d, $J = 8.9$), 8.02 (2H, d, $J = 8.9$), 3.21 (1H, d, $J = 13.6$ Hz), 2.53 (1H, d, $J = 14.0$ Hz), 2.05 (1H, m), 1.85 (3H, m), 1.06–1.15 (3H, m), 0.68 (9H, s), ^{13}C NMR: δ 169.95, 161.63, 149.91, 134.30, 130.04, 123.00, 46.04, 31.80, 31.23, 26.89, 26.86, 26.40, 26.04, IR ν_{max}: 3098, 2959, 2865, 1741, 1638, 1615, 1528, 1440, 1367, 1343, 879 cm^{-1}. HRMS (ESI): Calcd $C_{17}H_{22}N_2O_4$ $[M+Na]^+$ 341.14718, found $[M+Na]^+$ 341.14735.

*4-tert-Butyl Cyclohexanone O-3,5-Dinitrobenzoyl Oxime (**4e**)*

Following the general procedure, oxime **4a** (275 mg, 1.62 mmol) in dichloromethane (8 mL) and pyridine (3 mL) was treated with 3,5-dinitrobenzoyl chloride (317 mg, 1.71 mmol) for 12 h to afford **4e** as a light brown solid (325 mg, 55 %), mp = 112.2–112.5°C. ^1H NMR: δ 9.12 (1H, d, $J = 2.0$ Hz), 9.04 (2H, bs), 3.33 (1H, d, $J = 13.6$ Hz), 2.67 (1H, d, $J = 6.2$ Hz), 2.21 (1H, m), 2.04 (3H, m), 1.30 (3H, m), 0.83 (9H, m), ^{13}C NMR: δ 171.24, 159.91, 148.24, 132.66, 128.84, 122.10, 46.56, 32.04, 31.37, 27.05, 27.02, 26.79, 26.25, IR ν_{max}: 3091, 2970, 2870, 1739, 1630, 1546, 1443, 1366, 1359, 867 cm^{-1}. HRMS (ESI): Calcd $C_{17}H_{21}N_3O_6$ $[M+Na]^+$ 386.13226, found $[M+Na]^+$ 386.13231.

*4-tert-Butyl Cyclohexanone O-3,4-Dinitrobenzoyl Oxime (**4f**)*

Following general procedure, oxime **4a** (0.4 g, 2.36 mmol) in dichloromethane (8 mL) and pyridine (2 mL) was treated with 3,4-dinitrobenzoyl chloride (572 mg, 2.48 mmol) for 11 h to afford **4f** as a brown solid (0.54 g, 63 %), mp = 122.9–124.1°C. ^1H NMR: δ 8.55 (1H, d, $J = 1.5$ Hz), 8.39 (1H, dd, $J = 8.4$, 1.5 Hz), 8.00 (1H, d, $J = 8.4$ Hz), 3.32 (1H, d, $J = 12.8$ Hz), 2.75 (1H, d, $J = 14.0$ Hz), 2.28–2.20 (1H, m), 2.07–2.00 (3H, m), 1.35–1.26 (3H, m), 0.89 (9H, m), ^{13}C NMR: δ 171.03, 159.99, 144.61, 141.99, 134.22, 134.00, 131.92, 125.22, 46.46, 40.72, 31.94, 31.30, 26.97, 26.63, 26.14, IR ν_{max}: 3098, 2970, 2956, 2870, 1738, 1604, 1542, 1440, 1365, 1350, 844 cm^{-1}. HRMS (ESI): Calcd $C_{17}H_{21}N_3O_6$ $[M+Na]^+$ 386.13226, found $[M+Na]^+$ 386.13236.

*4-tert-Butyl Cyclohexanone O-2-Nitrobenzoyl Oxime (**4g**)*

To a solution of oxime **4a** (0.40 g, 2.36 mmol) in dichloromethane (7 mL) was added pyridine (2 mL).The mixture was stirred for 30 min before 2-nitrobenzoyl chloride (460 mg, 2.48 mmol) was added at 0°C. The reaction was refluxed for 12 h and worked up to afford **4g** as a yellow solid (0.58 g, 77 %), mp = 71.9–73.4°C. ^1H NMR: δ 7.70 (1H, dd, $J = 7.0$, 7.0 Hz), 7.51 (2H, d, $J = 7.0$ Hz), 7.46 (1H, m), 2.90 (1H, d, $J = 12.0$ Hz), 2.35 (1H, bs), 1.93 (1H, m), 1.92 (1H, bs), 1.89–1.59 (1H, m), 1.01–0.89 (3H, m), 0.59 (9H, s), ^{13}C NMR: δ 169.54, 162.70, 147.06, 132.62, 131.34, 129.21, 125.86, 123.09, 46.01, 31.46, 30.82, 26.63, 26.57, 25.90, 25.70, IR ν_{max}: 3085, 2959, 2870, 1749, 1639, 1612, 1579, 1533, 1445, 1366, 1350, 856 cm^{-1}. HRMS (ESI): Calcd $C_{17}H_{22}N_2O_4$ $[M+Na]^+$ 341.14718, found $[M+Na]^+$ 341.14722.

*4-tert-Butyl Cyclohexanone O-2,4-Dinitrobenzoyl Oxime (**4h**)*

Following general procedure, oxime **4a** (360 mg, 2.13 mmol) in dichloromethane (5 mL) and pyridine (2 mL) was treated with 2,4-dinitrobenzoyl chloride (515 mg, 2.23 mmol) for 15 h to afford **4h** as a brown oil (490 mg, 63 %). ^1H NMR: δ 8.63 (1H, d, $J = 2.2$ Hz), 8.45 (1H, dd, $J = 8.4$, 2.2 Hz), 7.86 (1H, d, $J = 8.4$ Hz,), 2.96 (1H, d, $J = 12.4$ Hz), 2.36 (1H, d, $J = 14.0$ Hz), 2.03–1.95 (1H, m), 1.86–1.69 (3H, m), 1.16–0.99 (3H, m), 0.67 (9H, s), ^{13}C NMR: δ 170.86, 162.33, 148.53, 147.17, 132.13, 131.13, 127.74, 119.14, 46.55, 32.03, 31.27, 27.20, 27.07, 26.54, 26.15, IR ν_{max}: 3107, 2957, 2869, 1748, 1614, 1603, 1535, 1365, 1346, 834 cm^{-1}. HRMS (ESI): Calcd $C_{17}H_{21}N_3O_6$ $[M+Na]^+$ 386.13226, found $[M+Na]^+$ 386.13236.

*4-tert-Butyl Cyclohexanone O-2,4,6-Trinitrophenyl Oxime (**4i**)*

Oxime **4a** (1 g, 0.591 mmol) in dichloromethane (10 mL) was treated with triethylamine (1.23 mL, 896 mg, 8.86 mmol) and 2,4,6-trinitrofluorobenzene (1.5 g, 6.50 mmol) to afford **4i** as a yellowish brown solid (1.16 g, 52 %), mp = 129.1–131.0°C. ^1H NMR: δ 8.73 (2H, s), 3.34 (1H, dd, $J = 14.2$, 2.0 Hz), 2.37 (1H, d, $J = 14.2$ Hz), 2.02–1.98 (3H, m), 1.28–1.22 (4H, m), 0.85 (9H, s), ^{13}C NMR: δ 170.67, 150.93, 141.96, 140.48, 124.04, 47.13, 32.63, 30.93, 27.79, 27.64, 27.01, 26.60, IR ν_{max}: 3093, 2956, 2869, 1603, 1539, 1345, 914 cm^{-1}. HRMS (ESI): Calcd $C_{16}H_{20}N_4O_7$ $[M+H]^+$ 381.14048, found $[M+H]^+$ 381.14049.

*4-tert-Butyl Cyclohexanone O-4-Toluenesulfonyl Oxime (**4j**)*

4-Toluenesulfonyl chloride (1.13 g, 5.91 mmol) was added to oxime **4a** (1.0 g, 0.591 mmol) in pyridine, over 20 min. The resultant mixture was stirred at 0 to −20°C for 3 h. The white precipitate in the mixture was filtered, washed accordingly, and dried to successfully give the desired product **4j** as white solid (1.45 g, 76 %), mp = 97.3–98.6°C. ^1H NMR: δ 7.83 (2H, d, $J = 9.2$ Hz), 7.49 (2H, d, $J = 9.2$ Hz), 3.17 (1H, d, $J = 6.2$ Hz), 2.43 (3H, s), 2.35 (1H, d, $J = 6.2$ Hz), 2.20–1.86 (4H, d, $J = 6.2$ Hz), 1.31 (1H, m), 1.18–0.7 (2H, m), 0.83 (9H, s), ^{13}C NMR: δ 170.56, 145.24, 133.53, 129.93, 128.88, 46.69, 32.24, 31.30, 29.48, 29.33, 29.17, 29.01, 20.98, IR ν_{max}: 3080, 2951, 2867, 1641, 1597, 1428, 1368, 1191, 753 cm^{-1}.

*(E)-2,2-Dimethylcyclohexanone Oxime (**5a**)*

A solution of hydroxylamine hydrochloride (1.551 g, 24.05 mmol) and sodium acetate (1.312 g, 16.03 mmol) in water (25 mL) and ethanol (5 mL) was warmed to 60°C and crude 2,2-dimethylcyclohexanone (2.02 g, 16.01 mmol) was added with swirling. The flask was stirred and ethanol was added until the solution became homogeneous (approximately 30 mL). The solution was further stirred at 60°C for 3 h, kept at ambient temperature overnight, then poured onto ice. The mixture was extracted with ether, concentrated, and crystallised from methanol to yield **5a** as white flakes (1.108 g, 7.846 mmol, 49 %), mp = 93–94°C. (lit. mp = 93.5–94°C).[34]

(E)-2,2-Dimethylcyclohexanone O-4-Nitrophenyl Oxime (**5b**)

Oxime **5a** (80 mg, 0.57 mmol) was added to a suspension of KH (46 mg, 1.15 mmol) in anhydrous THF (20 mL). The solution was stirred for 30 min at room temperature then cooled to 0°C before a solution of 1-fluoro-4-nitrobenzene (120 mg, 0.85 mmol) in anhydrous THF (20 mL) was added and the reaction was stirred at room temperature for 18 h. The reaction was quenched with H_2O (10 mL), diluted with ether (50 mL), then washed with H_2O (3×100 mL). The organic layer was dried ($MgSO_4$), filtered, and concentrated to afford **5b** as colourless plates (136 mg, 91 %), mp = 65.1–67.0°C. ^{1}H NMR: δ 8.20 (2H, d, $J = 7$ Hz), 7.26 (2H, d, $J = 9$ Hz), 1.69 (4H, m), 1.43 1H, s), 1.61 (3H, m), 1.26 (6H, s), ^{13}C NMR: δ 171.1, 164.7, 141.9, 125.7, 114.2, 41.3, 38.4, 26.7, 26.2, 22.6, 21.5, IR ν_{max}: 2920, 1587 cm^{-1}. HRMS (ESI): Calculated for $C_{14}H_{19}NO_3^+$ [M+H]$^+$ 263.1390, found 263.1390.

(E)-2,2-Dimethylcyclohexanone O-3-Nitrobenzoyl Oxime (**5c**)

By the standard procedure oxime **5a** (80 mg, 0.57 mmol) in dichloromethane (20 mL) and pyridine (2 mL) was treated with 3-nitrobenzoyl chloride (159 mg, 0.86 mmol) to afford **5c** (124 mg, 0.43 mmol, 75 %), which was recrystallized from MeOH to give colourless plates, mp = 95.8–97.1°C. ^{1}H NMR: δ 8.83 (1H, s), 8.42 (1H, m), 8.34 (1H, m), 7.68 (1H, m), 1.5–1.6 (6H, m), 2.69 (2H, m), 1.29 (6H, s), ^{13}C NMR: δ 175.8, 162.2, 148.3, 135.2, 131.5, 129.7, 127.4, 124.3, 41.2, 38.9, 26.6, 26.2, 23.6, 21.3, IR ν_{max}: 2954, 1741, 1530 cm^{-1}. HRMS (ESI): Calculated for $C_{15}H_{19}N_2O_4^+$ [M+H]$^+$ 291.1339, found 291.1339.

(E)-2,2-Dimethylcyclohexanone O-3,4-Dinitrobenzoyl Oxime (**5e**)

By the standard procedure oxime **5a** (70 mg, 0.50 mmol) in CH_2Cl_2 (20 mL) and pyridine (2 mL) was treated with 3,4-dinitrobenzoyl chloride (175 mg, 0.76 mmol) to afford **5e** (144 mg, 86 %), which was recrystallized from MeOH to give colourless plates, mp = 129.1–130.7°C. ^{1}H NMR: δ 8.55 (1H, d, $J = 1.7$ Hz), 8.42 (1H, dd, $J = 8.3$, 1.7 Hz), 8.00 (1H, d, $J = 8.3$ Hz), 2.67 (2H, t, $J = 13$ Hz), 1.71 (4H, m), 1.66 (2H, t, $J = 11$ Hz), 1.30 (6H, s), ^{13}C NMR: δ 176.6, 160.4, 145.1, 142.6, 134.3, 126.0, 125.4, 41.2, 39.1, 26.5, 26.2, 23.8, 21.3, IR ν_{max}: 2956, 1745, 1543 cm^{-1}.

(E)-2,2-Dimethylcyclohexanone O-3,5-Dinitrobenzoyl Oxime (**5f**)

By the standard procedure oxime **5a** (80 mg, 0.57 mmol) in dichloromethane (20 mL) and pyridine (2 mL) was treated with 3,5-dinitrobenzoyl chloride (201 mg, 0.87 mmol) to afford **5f** (130 mg, 68 %), which was recrystallized from MeOH to give colourless plates, mp = 102.4–103.8°C. ^{1}H NMR: δ 9.24 (1H, dd, $J = 2$, 2 Hz), 9.15 (2H, d, $J = 2$ Hz,), 2.70 (2H, m), 1.6–1.8 (6H, m). 1.32 (6H, s), ^{13}C NMR: δ 175.6, 164.3, 148.6, 147.2, 133.8, 130.8, 128.0, 119.2, 41.1, 38.7, 26.2, 26.1, 23.4, 21.2, IR ν_{max}: 2938, 1743, 1542 cm^{-1}. HRMS (ESI): Calculated for $C_{15}H_{17}N_3O_6^+$ [M+H]$^+$ 336.1190, found 336.1189.

(E)-2,2-Dimethylcyclohexanone O-2-Nitrobenzoyl Oxime (**5g**)

By the standard procedure oxime **5a** (80 mg, 0.57 mmol) in CH_2Cl_2 (20 mL) and pyridine (2 mL) was treated with 2-nitrobenzoyl chloride (159 mg, 0.86 mmol) giving **5g** (137 mg, 83 %), which was recrystallized from MeOH to give colourless needles, mp = 79.6–82.0°C. ^{1}H NMR: δ 8.00 (1H, d, $J = 8$ Hz) 7.60–7.75 (3H, m), 2.53 (2H, m), 1.55–1.66 (6H, m), 1.14 (6H, s, C**H$_3$**), ^{13}C NMR: δ 175.1, 165.0, 147.5, 133.4, 133.4, 131.3, 129.8, 127.9, 123.7, 41.2, 38.7, 26.3, 26.1, 23.4, 21.3, IR ν_{max}: 2938, 1728, 1540 cm^{-1}. HRMS (ESI): Calculated for $C_{15}H_{19}N_2O_4^+$ [M+H]$^+$ 291.1339, found 291.1340.

(E)-2,2-Dimethylcyclohexanone O-2,4-Dinitrobenzoyl Oxime (**5h**)

By the standard procedure oxime **5a** (80 mg, 0.57 mmol) in dichloromethane (20 mL) and pyridine (2 mL) was treated with 2,4-dinitrobenzoyl chloride (200 mg, 0.87 mmol) to afford **5h** (151 mg, 0.45 mmol, 79 %), which was recrystallized from MeOH to give colourless plates, mp = 122.8–123.7°C. ^{1}H NMR: δ 8.88 (1H, d, $J = 2.2$ Hz), 8.57 (1H, dd, $J = 8.4$, 2.2 Hz), 7. 89 (1H, d, $J = 8.4$ Hz), 2.55 (2H, t, $J = 12.5$ Hz), 1.63 (4H, m), 1.53 (2H, t, $J = 11$ Hz), 1.07 (6H, s), ^{13}C NMR: δ 176.7, 160.3, 148.7, 133.5, 129.2, 122.4, 41.2, 39.1, 26.6, 26.2, 23.8, 21.3, IR ν_{max}: 2934, 1740, 1532 cm^{-1}. HRMS (ESI): Calculated for $C_{15}H_{17}N_3O_6^+$ [M+H]$^+$ 336.1191, found 336.1189.

References

[1] (a) H. B. Burgi, J. D. Dunitz, E. Shefter, *J. Am. Chem. Soc.* **1973**, *95*, 5065. doi:10.1021/JA00796A058
(b) Structure Correlation, ed. H. B. Burgi and J. D. Dunitz, **1994**, vol. 1 and 2 (Verlag Chemie: Weinheim).

[2] (a) F. H. Allen, R. Mondalb, N. A. Pitchford, J. A. K. Howard, *Helv. Chim. Acta* **2003**, *86*, 1129. doi:10.1002/HLCA.200390098
(b) T. P. E. A. Derheyde, L. R. Nassimbeni, *Acta Cryst. A* **1984**, *40*, SC104.

[3] V. Ferretti, V. Bertolasi, P. Gilli, G. Gilli, *Phys. Chem. Chem. Phys.* **1999**, *1*, 2303. doi:10.1039/A900592G

[4] S. A. Jackson, O. Eisenstein, J. D. Martin, A. C. Albeniz, R. H. Crabtree, *Organometallics* **1991**, *10*, 3062. doi:10.1021/OM00055A019

[5] L.-K. Liu, C.-H. Sun, C.-Z. Yang, Y.-S. Wen, C.-F. Wu, S.-S. Shih, K.-S. Lin, *Organometallics* **1992**, *11*, 972. doi:10.1021/OM00038A074

[6] (a) T. Auf der Heyde, *Angew. Chem. Int. Ed. Engl.* **1994**, *33*, 823. doi:10.1002/ANIE.199408231
(b) S. N. Tandura, S. N. Gurkova, A. I. Gusev, N. V. Alekseev, *Zh. Strukt. Khim* **1985**, 136.

[7] (a) A. R. Bassindale, D. J. Parker, P. G. Taylor, N. Auner, B. Herrschaft, *J. Organomet. Chem.* **2003**, *667*, 66. doi:10.1016/S0022-328X(02)02130-7
(b) G. Klebe, *J. Organomet. Chem.* **1985**, *293*, 147. doi:10.1016/0022-328X(85)80283-7

[8] A. G. Orpen, I. D. Salter, *Organometallics* **1991**, *10*, 111. doi:10.1021/OM00047A037

[9] (a) D. J. Hankinson, J. Almloef, K. R. Leopold, *J. Phys. Chem.* **1996**, *100*, 6904. doi:10.1021/JP960353D
(b) M. A. Dvorak, R. S. Ford, R. D. Suenram, F. J. Lovas, K. R. Leopold, *J. Am. Chem. Soc.* **1992**, *114*, 108. doi:10.1021/JA00027A015

[10] (a) M. Kaftory, D. A. Nugiel, S. E. Biali, Z. Rappoport, *J. Am. Chem. Soc.* **1989**, *111*, 8181. doi:10.1021/JA00203A019
(b) G. A. Sim, *Acta Crystallogr. B* **1990**, *46*, 676. doi:10.1107/S0108768190006802
(c) Z. Rappoport, S. E. Biali, M. Kaftory, *J. Am. Chem. Soc.* **1990**, *112*, 7742. doi:10.1021/JA00177A039

[11] (a) D. Birney, T. K. Lim, J. Peng, B. R. Pool, J. M. White, *J. Am. Chem. Soc.* **2002**, *124*, 5091. doi:10.1021/JA025634F
(b) B. R. Pool, J. M. White, *Org. Lett.* **2000**, *2*, 3505. doi:10.1021/OL006553W

(c) Y. W. Goh, J. M. White, *Aust. J. Chem.* **2009**, *62*, 419. doi:10.1071/CH09358

(d) Y. W. Goh, B. R. Pool, J. M. White, *J. Org. Chem.* **2008**, *73*, 151. doi:10.1021/JO7018575

(e) Y. W. Goh, J. M. White, *Org. Biomol. Chem.* **2007**, *5*, 2354. doi:10.1039/B707643F

(f) Y. W. Goh, S. M. Danczak, T. K. Lim, J. M. White, *J. Org. Chem.* **2007**, *72*, 2929. doi:10.1021/JO0625610

(g) J. Roth-Barton, Y. W. Goh, A. Karnezis, J. M. White, *Aust. J. Chem.* **2009**, *62*, 407. doi:10.1071/CH09349

(h) J. Roth-Barton, J. M. White, *Aust. J. Chem.* **2009**, *62*, 1695. doi:10.1071/CH09349

[12] Y. W. Goh, J. M. White, *Org. Biomol. Chem.* **2005**, *3*, 972. doi:10.1039/B417538G

[13] H.-X. Wei, C. Zhou, S. Ham, J. M. White, D. M. Birney, *Org. Lett.* **2004**, *6*, 4289. doi:10.1021/OL048197D

[14] (a) M. R. Edwards, P. G. Jones, A. J. Kirby, *J. Am. Chem. Soc.* **1986**, *108*, 7067. doi:10.1021/JA00282A036

(b) P. G. Jones, A. J. Kirby, *J. Am. Chem. Soc.* **1984**, *106*, 6207. doi:10.1021/JA00333A015

[15] (a) P. G. Jones, M. R. Edwards, A. J. Kirby, *Acta Crystallogr. C* **1986**, *42*, 1230. doi:10.1107/S0108270186092788

(b) M. R. Edwards, A. J. Kirby, P. R. Raithby, P. G. Jones, *Acta Crystallogr. C* **1987**, *43*, 300. doi:10.1107/S0108270187096057

[16] R. Gawley, Beckman Reactions in *Organic Reactions,* **1988**, pp. 1–420 (Hoboken, NJ).

[17] W. J. Bailey, M. Madoff, *J. Am. Chem. Soc.* **1954**, *76*, 2707. doi:10.1021/JA01639A033

[18] D. R. Lide, *CRC Handbook of Chemistry and Physics*, 79th Ed., **1998** (CRC Press LLC: Florida).

[19] J. A. Dean, *Lange's Handbook of Chemistry*, 14th Ed., **1992** (McGraw-Hill: New York).

[20] J. F. King, *Sulphonic Acids, Esters and Their Derivatives, Chap. 6*, **1991**, pp. 249–259 (John Wiley & Sons: New York).

[21] F. J. Hoogesteger, L. W. Jenneskins, H. Kooijman, N. Veldman, A. L. Spek, *Tetrahedron* **1996**, *52*, 1773. doi:10.1016/0040-4020(95)01012-2

[22] C. Glidewell, J. N. Low, J. M. S. Skakle, J. L. Wardell, *Acta Crystallogr. C* **2004**, *60*, 270. doi:10.1107/S0108270104004299

[23] M. Lutz, A. L. Spek, R. Dabiron, C. A. von Walree, L. W. Jenneskens, *Acta Crystallogr. C* **2004**, *60*, 127. doi:10.1107/S0108270103029196

[24] (a) R. J. Gillespie, *J. Chem. Educ.* **1963**, *40*, 295. doi:10.1021/ED040P295

(b) R. J. Gillespie, *Ed. Quim.* **2006**, *17*, 264.

(c) R. J. Gillespie, *Coord. Chem. Rev.* **2008**, *252*, 1315. doi:10.1016/J.CCR.2007.07.007

[25] (a) A. J. Briggs, R. Glenn, P. G. Jones, A. J. Kirby, P. Ramaswamy, *J. Am. Chem. Soc.* **1984**, *106*, 6200. doi:10.1021/JA00333A014

(b) R. D. Amos, N. C. Handy, P. G. Jones, A. J. Kirby, J. K. Parker, J. M. Percy, M. D. Su, *J. Chem. Soc., Perkin Trans. 2* **1992**, 549. doi:10.1039/P29920000549

(c) B. R. Pool, J. M. White, P. P. Wolynec, *J. Org. Chem.* **2000**, *65*, 7595. doi:10.1021/JO0055638

(d) W. Jackson, J. M. White, *Aust. J. Chem.* **2008**, *61*, 956. doi:10.1071/CH08402

(e) A. J. Green, J. Giordano, J. M. White, *Aust. J. Chem.* **2000**, *53*, 285. doi:10.1071/CH99138

[26] J. M. White, M. Spiniello, *Org. Biomol. Chem.* **2003**, *1*, 3094.

[27] (a) C. J. Unkefer, R. E. London, T. W. Whaley, G. H. Daub, *J. Am. Chem. Soc.* **1983**, *105*, 733. doi:10.1021/JA00342A010

(b) P. E. Hansen, *Annu. Rep. NMR Spectrosc.* **1981**, *11A*, 65. doi:10.1016/S0066-4103(08)60409-3

(c) P. E. Hansen, O. K. Poulsen, A. Berg, *Org. Magn. Reson.* **1979**, *12*, 43. doi:10.1002/MRC.1270120110

(d) J. L. Marshall, A. M. Ihrig, D. E. Miller, *J. Magn. Reson.* **1974**, *16*, 439.

(e) S. Berger, K. P. Zeller, *J. Chem. Soc. D* **1975**, 423.

[28] G. R. Jones, S. Caldarelli, P. Vogel, *Helv. Chim. Acta* **1997**, *80*, 59. doi:10.1002/HLCA.19970800105

[29] (a) R. R. Fraser, R. Capoor, J. W. Bovenkamp, B. V. Lacroix, J. Pagotto, *Can. J. Chem.* **1983**, *61*, 2616. doi:10.1139/V83-448

(b) L. B. Krivdin, G. A. Kalabin, R. N. Nesterenko, B. A. Trofimov, *Tetrahedron Lett.* **1984**, *25*, 4817. doi:10.1016/S0040-4039(01)81528-8

(c) L. B. Krivdin, G. A. Kalabin, *Prog. Nucl. Magn. Reson. Spectrosc.* **1989**, *21*, 293. doi:10.1016/0079-6565(89)80007-X

(d) F. J. Hoogesteger, D. M. Grove, L. W. Jenneskens, T. J. M. de Bruin, B. A. J. Jansen, *J. Chem. Soc., Perkin Trans. 2* **1996**, 2327. doi:10.1039/P29960002327

[30] N. A. Shcherbina, N. V. Istomina, L. B. Krivdin, *Zh. Org. Khim* **2005**, *41*, 1127.

[31] G. M. Sheldrick, *Acta Crystallogr. A* **2008**, *64*, 112. doi:10.1107/S0108767307043930

[32] L. J. Farrugia, *J. Appl. Cryst.* **1997**, *30*, 565. doi:10.1107/S0021889897003117

[33] L. J. Farrugia, *J. Appl. Cryst.* **1999**, *32*, 837. doi:10.1107/S0021889899006020

[34] G. N. Barber, R. A. Olofson, *J. Org. Chem.* **1978**, *43*, 3015. doi:10.1021/JO00409A017